Arabian Journal of Chemistry (2021) **14**, 103160

King Saud University

Arabian Journal of Chemistry

www.ksu.edu.sa
www.sciencedirect.com

ORIGINAL ARTICLE

Adsorption of phenol and chromium (VI) from aqueous solution using exfoliated graphite: Equilibrium, kinetics and thermodynamic studies

Siyabulela J. Tshemese [a], **Washington Mhike** [b], **Shepherd M. Tichapondwa** [a]

[a] *Department of Chemical Engineering, University of Pretoria, Pretoria 0002, South Africa*
[b] *Department of Chemical, Metallurgical and Materials Engineering (Polymer Technology Division), Tshwane University of Technology, Pretoria 0183, South Africa*

Received 15 February 2021; accepted 8 April 2021
Available online 16 April 2021

KEYWORDS

Adsorption;
Chromium (VI);
Exfoliated Graphite;
Phenol

Abstract Several industrial effluents contain Cr (VI) and phenol in varying concentrations. These compounds are highly toxic even at low concentrations. In this study, Exfoliated Graphite (EG) was investigated as an adsorbent towards the removal of these contaminants. This was motivated by its availability, ease of synthesis and high surface area. The exfoliation process resulted in graphite that had a worm-like accordion structure and an increased surface area from 2.4 to 22.4 m^2g^{-1}. The optimum loading for both pollutants was 30 g/L and equilibrium was attained in a 48 h period. Maximum Cr (VI) removal (89.8%) occurred under acidic conditions (pH 2) while phenol was preferentially removed (62.3%) under basic environments (pH 12). Three non-linear adsorption models, namely Redlich-Peterson, Freundlich and Langmuir were evaluated. The Redlich-Peterson isotherm, with an exponential constant, $\beta = °0.8982$ best described the equilibrium data for Cr (VI) with a regression coefficient of $R^2 = °0.9965$ while the Langmuir isotherm accurately described the phenol adsorption with a regression coefficient of $R^2 = °0.9975$. The pseudo-second order rate equation adequately represented the experimental data for phenol and Cr (VI) with regression coefficients greater than 0.99. Adsorption thermodynamic studies revealed that the attachment of phenol and Cr (VI) onto EG was a feasible, endothermic and spontaneous process.

1. Introduction

The World Health Organization (WHO) reports that approximately 80% of the world's wastewater is left untreated. This exposes many communities to the risk of utilizing contaminated water supplies resulting in diseases and disruptions to economic activities. The major sources of wastewater include industrial effluents and domestic discharge (Naidoo and

E-mail address: shepherd.tichapondwa@up.ac.za (S.M. Tichapondwa)
Peer review under responsibility of King Saud University.

Production and hosting by Elsevier

https://doi.org/10.1016/j.arabjc.2021.103160
1878-5352

Olaniran, 2013). Effluent from industries such as mining, petroleum, leather tanning and pigment manufacturing have been reported to contain heavy metals such as chromium (VI) and phenolic pollutants (Gładysz-Płaska et al., 2012, Gupta and Balomajumder, 2015, Li et al., 2016). Both these contaminants are identified as priority pollutants by the Environmental Protection Agency (EPA) (Huang et al., 2007, Li et al., 2016) with high toxicity being observed even at low concentrations. Both pollutants tend to bio-accumulate (Nagy et al., 2017) and may pose health risks to humans and animals and can be toxic to aquatic life if left untreated. To avoid these deleterious effects, it is imperative that these pollutants be removed or reduced to below acceptable levels before wastewater can be returned to water bodies.

Several treatment methods for the remediation of these pollutants have been employed. These include photocatalytic oxidation (Tshuto et al., 2017), oxidation–reduction (Diao et al., 2016), membrane processes (Won et al., 2012) and adsorption (Gładysz-Płaska et al., 2012). Adsorption is considered as one of the most practical methods of removing pollutants from aqueous media due to the low cost, easy handling, high efficiency and environmentally friendliness associated with the technology (Foo and Hameed, 2010, Kundu and Gupta, 2006, Gładysz-Płaska et al., 2012). Various adsorbents such as clay materials (Huang et al., 2008a, Huang et al., 2008b, Gładysz-Płaska et al., 2012, Tichapondwa and Van Biljon, 2019), activated carbon (Ji et al., 2009, Ravulapalli and Kunta, 2018, Lütke et al., 2019), soil (Subramanyam and Das, 2009), zeolite (Li et al., 2015), sawdust (Meniai, 2012), graphene (Li et al., 2012), polymer materials (Yu et al., 2013, Makrigianni et al., 2015, Tshemese et al., 2020), carbon nanotubes (Huang et al., 2015) and honeycomb carbon materials (Liang et al., 2019) have been used to remediate phenol and Cr (VI). Their use is motivated by the high surface area, high cation exchange capacity and high affinity towards these pollutants. The advantages of these adsorbents include easy synthesis and low cost while the disadvantage particularly for activated carbon remains regeneration onsite.

Exfoliated graphite is obtained through the vaporization of intercalation compounds present in expandable graphite (Chung, 2015), this results in a material with low density, porous structure and high surface area. The highly oxidative intercalation procedure used to prepare expandable graphite and the subsequent thermal treatment process utilized to exfoliate it (either furnace or microwave) result in the occurrence of oxygen functional groups on the exfoliated graphite due to partial oxidation (Chung, 2015). These functional groups together with its high surface area have resulted in EG being applied as an adsorbent in pollutant remediation studies (Tichapondwa et al., 2018, Van Pham et al., 2020). Carvallho et al. (2016) and Van Pham et al. (2019) used exfoliated graphite for the removal of blue textile dyes and Congo red, respectively. However, the adsorption of phenol and Cr (VI) using EG is yet to be fully explored. Our previous work reported preliminary findings on the efficiency of EG as an adsorbent to these pollutants (Tichapondwa et al., 2018). The present study aims to expand on these initial studies by investigating the optimal adsorption parameters and establishing the kinetics and thermodynamic parameters.

2. Material and methods

2.1. Materials

In order to obtain the exfoliated graphite, Grade ES250 B5 expandable graphite (Qingdao Kropfmeuhl Graphite) was exposed to a temperature shock at 600 °C for at least 5 min in a Thermo-power electric furnace (Focke et al., 2014). Potassium chromate and sodium hydroxide were obtained from Merck (Germany) while phenol and 1.5-diphenylcarbazide were obtained from Saarchem and Sigma-Aldrich (South Africa), respectively. Hydrochloric acid was supplied by Glassworld, South Africa.

2.2. Batch adsorption studies

Aqueous Cr (VI) and phenol solutions with varying concentrations were made by diluting appropriate volumes of 1000 mg/L stock solutions with deionized water. The optimum adsorbent loading was determined by using 5 to 30 g/L of EG and contacting it with 30 mg/L of Cr(VI) or phenol solutions for 48 h. The effect of initial pH on the removal of the pollutants was studied in the 2 to 12 pH range. The pH was altered with hydrochloric acid and sodium hydroxide. Adsorption isotherms were determined at the optimum conditions for each pollutant, and the concentration was varied from 10 to 100 mg/L. The kinetics were determined by drawing an appropriate sample volume at pre-determined time intervals and filtering before analysis.

2.3. Phenol and Cr (VI) analysis

Changes in Cr (VI) concentration were tracked using the standard colorimetric method detailed in our previous work (Tichapondwa et al. 2018). The phenol concentration was determined using high performance liquid chromatography. The phenol separation was performed on a Waters PAH C18 (4.6 × 250 mm, 5 μL) column and the resultant data was analysed using proprietary Empower software. The mobile phase was composed of two solvents namely, a 1% acetic acid and water mixture and a 1% acetic acid in acetonitrile mixture.

2.4. Characterization of materials

The surface morphology of EG before and after contact with the respective pollutants were viewed on a Zeiss Ultra Plus field emission scanning electron microscope (FEG SEM). The nature of the phases in the adsorbent material was determined through X-ray diffraction (XRD) measurements which were recorded using a Bruker D8 Advanced solid powder diffraction fitted with Lynx eye detector. The surface area was determined using a Micrometrics TriStar BET analyser. A ca. 7-fold increase from 2.4 to 22.4 m^2g^{-1} was observed upon exfoliation (Tichapondwa et al., 2018).

2.5. Equilibrium study

The equilibrium adsorption capacity $q_e\left(\frac{mg}{g}\right)$ was calculated using equation (1) (Belhachemi and Addoun, 2011) with V

(L) and W (g) the volume of the solution and mass of the EG respectively.

$$q_e = \frac{(C_0 - C_e)V}{W} \tag{1}$$

The Redlich-Peterson, Freundlich and Langmuir isotherms were adopted to evaluate the removal process. Equation (2) gives the Langmuir isotherm withQ_0 (mg/g) the maximum amount of a pollutant that EG can adsorb andK_L (L/mg) is the Langmuir constant.

The Langmuir isotherm assumes a homogeneous, monolayer adsorption mechanism (Riahi Samani et al., 2016). It was then assumed that once a Cr (VI) or a phenolate ion attaches on a site, no further attachment can take place on the occupied area.

$$q_e = Q_0 \frac{K_L C_e}{1 + K_L C_e} \tag{2}$$

The Freudlich isotherm is an empirical equation formulated to accurately predict the behavior of heterogeneous systems. The isotherm implies that an infinite attachment of pollutant molecules can take place (Foo and Hameed, 2010). The isotherm also deals with non-ideal and reversible adsorption (Singh et al., 2018). A higher n value means a lower affinity. The closer the value of n to zero, means that the system is heterogeneous. A value of n typically shows the degree of non-linearity with values of $n < 1$ indicating that the adsorption is a chemical process (Desta, 2013). The Freudlich model is given in equation (3) whereK_F , is the Freundlich constant and 1/n indicates the heterogeneity of the EG's surface.

$$q_e = K_F C_e^{\frac{1}{n}} \tag{3}$$

The Redlich-Peterson isotherm is an empirical equation with 3 parameters that include features from Langmuir and Freundlich isotherms (Singh et al., 2018) and can also be employed to predict adsorption equilibria. The Redlich-Peterson model is given in equation (4) whereK_{RP},$\propto_{RP}$ and β are the Redlich-Peterson constants. When$\beta = 1$ this equation becomes Langmuir and when$\beta = 0$ it becomes Henry's law equation.

$$q_e = \frac{K_{RP} Ce}{1 + \propto_{RP} C_e^{\beta}} \tag{4}$$

Due to inherent errors brought about by using linearized models for the isotherms, a non-linear regression method has been applied using the built-in function (solver) in Microsoft excel 2013 to determine the isotherm constants. In this study, the two error functions, sum of the squares of errors (ERRSQ) and Marquardt's percent standard deviation (MPSD) were employed to accurately predict the constants.

The ERRSQ in equation (5) is common and preferred by many researchers for its simplicity (Gimbert et al., 2008).

$$ERRSQ = \sum_{i=1}^{p} (q_{e,calc} - q_{e,meas})^2 \tag{5}$$

Equation (6) gives the MPSD error function. The smaller the MPSD value the more accurate the estimation ofq_e (Kumar et al., 2008).

$$MPSD = 100 \times \left(\sqrt{\frac{1}{n-p} \sum_{i=1}^{p} \left[\frac{(q_{e,calc} - q_{e,meas})^2}{q_{e,meas}}\right]_i}\right. \tag{6}$$

The kinetic behaviour of this adsorption process was evaluated using kinetic models, namely pseudo second order, Elovich's rate equation and pseudo first order. The pseudo first order rate equation describes a dynamic process of the liquid–solid phase adsorption (Dehghani et al., 2016). Equation (7) gives the linear form of Lagergren's rate equation whereq_e andq_t (mg/g) are the equilibrium adsorption capacities with time,$t(min)$ and$k_{p1}\left(min^{-1}\right)$ the pseudo first order rate constant.

$$\log(q_e - q_t) = \log q_e - \frac{k_{p1}}{2.303} t \tag{7}$$

The adsorption studies of various pollutants have been successfully projected using the widely used pseudo second order rate equation also known as the Ho's equation (Qiu et al., 2009). The linear form of the equation is detailed in equation (8) with$V_0 = k_{p2} q_e^2 \left(\frac{mg}{g.min}\right)$ which gives the initial adsorption rate.

$$\frac{t}{q_t} = \frac{1}{V_0} + \frac{1}{q_e} t \tag{8}$$

Elovich's equation describes the kinetics where chemisorption is the dominant force between the adsorbates and solids with heterogeneous sites. This equation over the years has seen its application extend to the liquid–solid adsorption processes. The linearized form of the Elovich equation is presented in equation (9) where$t_0 = \frac{1}{\propto a}$,$\propto$ is the initial adsorption rate and a is the desorption constant (Qiu et al., 2009).

$$q_t = \left(\frac{2.3}{\alpha}\right) \log(t + t_0) - \left(\frac{2.3}{\alpha}\right) \log t_0 \tag{9}$$

Liquid-solid adsorption processes are characterised by film diffusion, intra-particle diffusion and mass transfer. Equation (10) gives the intra-particle diffusion model used in the present study where$k_{int}$is the intra-particle diffusion rate constant.

$$q_t = k_{int} t^{\frac{1}{2}} + I$$

For the thermodynamic study, isotherm data were obtained at 25, 45 and 65 °C. A magnetic stirrer fitted with a temperature controller was used to maintain the target temperature within a ±2 °C range.

3. Results and discussion

3.1. Characterization of exfoliated graphite

The scanning electron microscope (SEM) micrographs of exfoliated graphite before adsorption, after contact with Cr (VI) and after contact with phenol are shown in Fig. 1. The surface of the EG prior to contact with either Cr (VI) or phenol is clear and smooth as shown in Fig. 1 (a) with the typical worm-like accordion structure. After contact with the respective pollutants, the initial worm-like structure collapses with smaller platelets breaking off from the main structure suggesting that

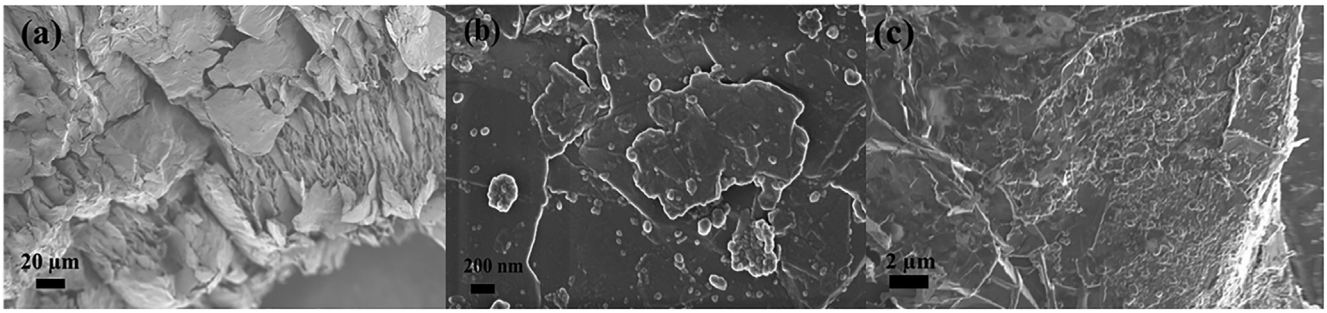

Fig. 1 The SEM images of (a) exfoliated graphite before adsorption studies (b) after Cr (VI) adsorption and (c) after phenol adsorption.

delamination of the EG into graphite nano-platelets occurred. The surface of EG became packed with visible spherical particles attached after Cr (VI) adsorption, Fig. 1(b) and even more packed after phenol adsorption Figure (c).

Qualitative XRD analysis was performed on the EG surface. Fig. 2 shows the XRD spectra of the EG prior to adsorption studies and compares it to the spectra after contacting with Cr (VI) and phenol, respectively. The main graphite peak was observed at a 2θ position of 30° for the samples before contact with phenol and Cr (VI) and after contact. This indicated the existence of graphitic structures in all samples (Ravulapalli and Kunta, 2018). Furthermore, the intensity of the peak increased after contacting the adsorbent with the respective pollutants. This confirms that EG delamination occurred after contacting it with the pollutants in aqueous solution. The resultant graphite nano-platelets had less imperfections and higher crystallinity compared to the EG, hence the sharper peaks.

3.2. Effect of adsorbent loading

The optimum EG loading resulting in maximum phenol and Cr (VI) removal was 30 g/L as shown in Fig. 3. The amount removed for phenol and Cr (VI) increased proportionally with an increase in the amount of adsorbent used before levelling off. Thereafter no noteworthy change in the amount removed was observed. It should also be noted that loadings beyond 30 g/L were not investigated due to mixing difficulties similar to those reported in our previous study (Tichapondwa et al., 2018). The increase in percentage pollutant removal with an increase in EG loading can be ascribed to the high number of adsorption sites active and available (Garg et al., 2007).

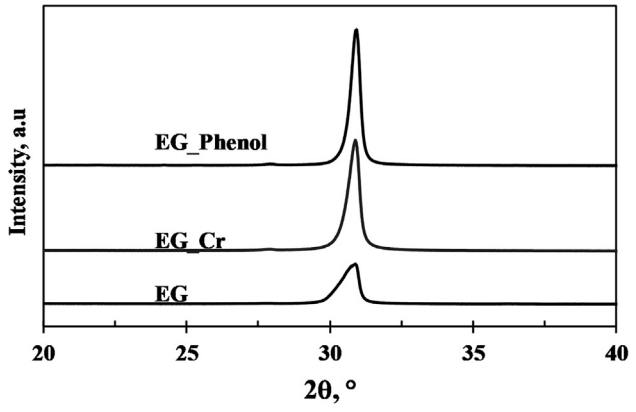

Fig. 2 XRD patterns for EG before and after contacting respective pollutants both at 10 mg/L.

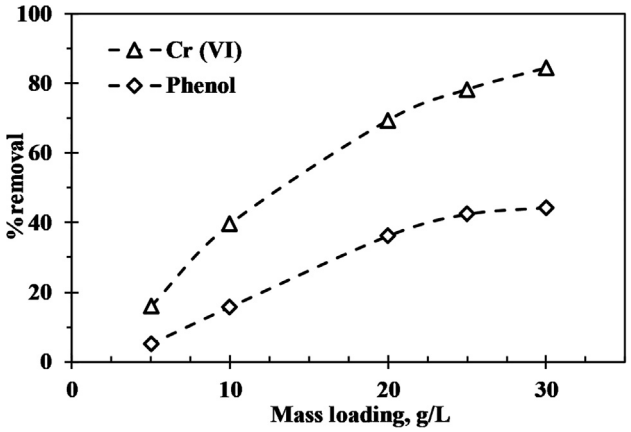

Fig. 3 Effect of adsorbent loading on pollutant removal C_o = 30-mg/L, 48 h.

3.3. Effect of pH

The initial pH of the aqueous medium affects the adsorption of both Cr (VI) and phenol since pH controls the surface charge of the adsorbent and degree of ionization of the adsorbate (Senturk et al., 2009). Fig. 4 shows the effect of solution pH on Cr (VI) and phenol removal by EG in the pH range 2 to 12. The maximum Cr (VI) removal (89.8%) was found under acidic conditions at pH 2. The amount of Cr (VI) removed decreased sharply after pH 7. This can be explained by considering the variation in the dominant Cr (VI) species with pH (Rakhunde et al., 2012) and (Szabó et al., 2018. According to Gładysz-Płaska et al. (2012), the prevalent form of Cr (VI) ions between pH 2 and 7 were $Cr_2O_7^{2-}$ and $HCrO_4^-$ ions whereas at pH values higher than 7, CrO_4^{2-} ions dominate. In the acidic region, the EG surface becomes positively charged due to strong protonation and attracts the negatively charged ions thus significantly enhancing adsorption (Gupta and Balomajumder, 2015). Above pH 7, it is assumed that there was a competition between CrO_4^{2-} and OH^- ions which resulted in the significant drop in the percentage pollutants removed. Similar observations have been reported by (Gupta and Balomajumder, 2015).

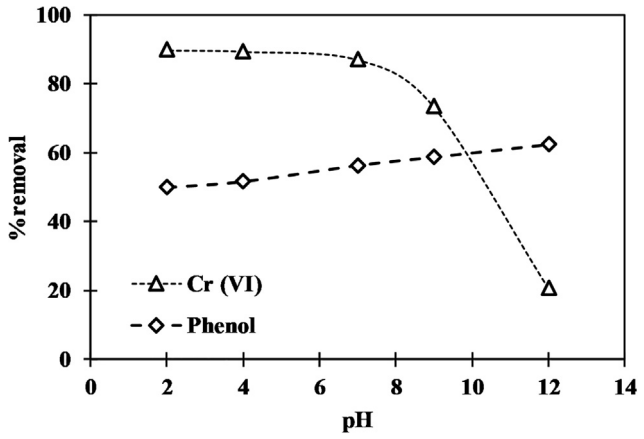

Fig. 4 Effects of pH on Cr (VI) and phenol removal at C_o = 30-mg/L of solution and 30 g/L loading respectively.

Phenol showed less affinity to EG than Cr (VI) and an increase in pH slightly improved the percentage removal of phenol from about 50% to just above 62% at pH 12. The amount of phenol removed was a weak function of the pH. This suggests that phenol removal was mainly due to the weak Van der Waals forces and weak pi bonds that exist between the phenol structure and the EG surface (Gupta and Balomajumder, 2015). Fig. 4 shows that increasing the value of pH increases the percentage of phenol removed. At pH < 7, the phenol molecule is mainly in its natural form, C_6H_5OH which is neutral and very stable and this negatively affected the adsorption process (Gładysz-Płaska et al., 2012, Ge et al., 2019). At pH greater than 7, the phenol molecule is largely in the form of the phenolate ion, $C_6H_5O^-$ and the strong base, OH^- ions in solution attract the H^+ ions forming water and leaving the adsorption sites for the phenolate ions (Ge et al., 2019). Ge et al. (2019) highlighted similar observations whilst using modified magadiite to absorb phenol.

It should also be noted that (Focke et al., 2014) who used the same precursor expandable graphite as the one used in this study confirmed the presence of oxygen functional groups on the exfoliated graphite. These functional groups were postulated to result from the partial oxidation of graphite during intercalation and exfoliation. During the intercalation process, the delocalized electrons in the conjugate pi orbitals of graphite interact with reacting species forming ionic compounds graphite salts. These, species can either donate electrons to graphite or accept electrons from graphite (Noel and Santhanam, 1998). For example, strong oxidizing agents will accept electrons from graphite to form acceptor compounds leading positively charged carbon layers on the graphite lattice. It is thus plausible that Cr (VI) in the form of the oxyanions interact with graphite this manner, during adsorption. Also, it has been reported that interactions exist between conjugated pi-electron electron systems (Wang et al., 2014; Yu et al., 2017). It is therefore plausible that the aromatic ring of phenol and graphite interact this manner (Yu et al., 2017; Tang et al., 2018). These mechanisms together with the contribution of the pH effects posited to be responsible for the removal of the target pollutants in the present study.

3.4. Adsorption isotherms

The mechanism of interaction between the adsorbates and the exfoliated graphite can be further elucidated by determining the equilibrium adsorption isotherms and kinetics of the systems. The model parameters were calculated by minimizing equation (5) and validated using equation (6). The results obtained through the fitting of the various adsorption isotherms to experimental data are presented in Fig. 5 while their corresponding constants are shown in Table 1. The Redlich-Peterson isotherm best described the Cr (VI) adsorption as confirmed by the regression coefficient °(R^{2° = 0.9965) and a low MPSD value (2.8532) obtained. A Redlich-Peterson exponential constant, β that lies between 0 and 1 indicates good adsorption (Gupta and Balomajumder, 2015). Fig. 5 (a) shows a close relationship between the fit of Langmuir and Redlich-Peterson models which can be attributed to the high exponential constant (β = 0.8982). As this constant approaches' unity, the Redlich-Peterson model reduces to the Langmuir model. For phenol adsorption, Fig. 5 (b), the Redlich-Peterson model reduced to the Langmuir model (β = 1). Several researchers (Aksu and Akpinar, 2000, Wong et al., 2004, Gimbert et al., 2008, Shahbeig et al., 2013) reiterated that the exponential constant cannot be greater than 1, hence this was used as a constraint in the solver function. Consequently, the Langmuir isotherms best describes the phenol adsorption on the EG with (R^2 = 0.9975) with a smaller MPSD value (MPSD = 9.3608). Parameters obtained from the Langmuir isotherm such as K_L were used to establish the separation factor (R_L) which indicates the likelihood of the adsorption process taking place. This separation factor is calculated using equation (11)

$$R_L = \frac{1}{1 + K_L C_0} \tag{11}$$

For$0 < R_L < 1$, the adsorption is favorable,$R_L > 1$, the adsorption is unfavorable, $R_L = 1$, adsorption is linear and $R_L = 0$, adsorption is irreversible (Belhachemi and Addoun, 2011, Gupta and Balomajumder, 2015). All theR_L values lie between 0 and 1 for both phenol and Cr (VI) and decrease as the concentration increases. This is indicative of a favorable adsorption process especially at lower concentration. TheR_L values of phenol are much higher than those of Cr (VI) for the same initial concentration suggesting that indeed the Langmuir model best describes the phenol adsorption when compared to the Cr (VI) adsorption. The Freundlich model resulted in the lowest regression coefficient values for phenol (R^2 = 0.9774) and Cr (VI) (R^2 = 0.9666) and which yielded the highest values of MPSD for phenol (MPSD = 30.98) and Cr (VI) (MPSD = 22.50) and suggesting a poor fit and no significant representation of the experimental data. The model assumes a heterogeneous system, which as proven by the heterogeneity factor is not true for this adsorption process since the heterogeneity factor for phenol and Cr (VI) is above 0.1. The current adsorption results have significantly improved from our initial results from an adsorption capacity of 0.55 mg/g and 0.73 mg/g to 2.14 mg/g and 2.23 mg/g for phenol and Cr (VI) respectively. This is mainly attributed to the optimized conditions of pH. Even though the results shows a good fit and high percentage removal, the adsorption capacity of the EG remains significantly lower as compared with other

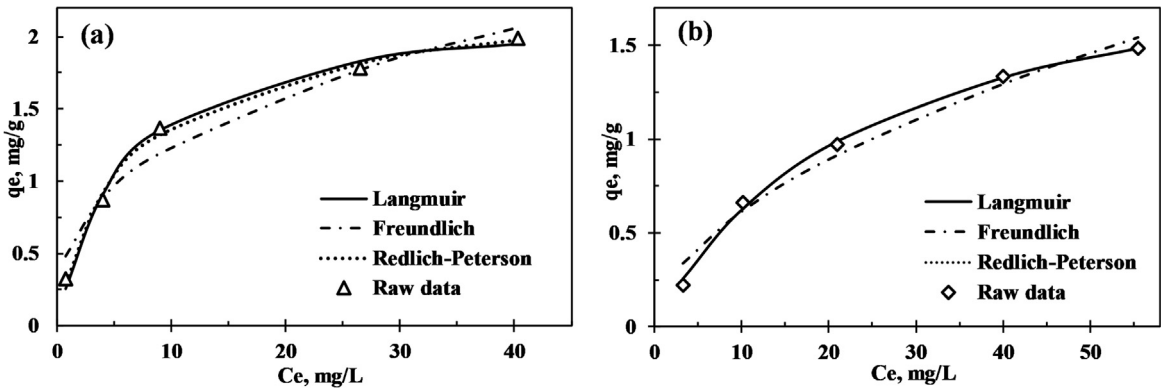

Fig. 5 Adsorption isotherms for (a) Cr (VI) at pH 2, adsorbent loading of 30 g/L and 48 h contact time and (b) Phenol at pH 12, adsorbent loading of 30 g/L and 48 h contact time.

Table 1 Parameters for the single components modelling for adsorption of Cr (VI) and phenol.

	Langmuir				Freundlich				Redlich				
	Q_0	K_L	MPSD	R^2	K_F	n	MPSD	R^2	K_{RP}	α_{RP}	β	MPSD	R^2
Cr (VI)	2.23	0.171	16.9	0.995	0.532	2.73	22.50	0.967	0.489	0.324	0.898	2.85	0.997
Phenol	2.14	0.041	9.36	0.998	0.178	1.86	30.98	0.977	0.088	0.041	1	11.5	0.998

adsorbents such as activated carbon (7.8 mg/g for Cr (VI) (Rai et al., 2016) and 98.6 mg/g for phenol (Lütke et al., 2019)), chitosan (12.4 mg/g for Cr (VI) (Ferrero et al., 2014)), polymer materials (500 mg/g for Cr (VI) (Yu et al., 2013), 51.92 mg/g for phenol (Makrigianni et al., 2015) as well as 38.2 mg/g for Cr (VI) (Tshemese et al., 2020)), clay materials (320.0 mg/g for Cr (VI) (Akram et al., 2017)), honeycomb carbon materials (332.5 mg/g for Cr (VI) (Liang et al., 2019)) and graphene (28.3 mg/g for phenol (Li et al., 2012)). The EG material however has adsorption capacity comparable to other adsorbents such as saw dust (3.7 mg/g for phenol (Meniai, 2012)), clay materials (4.3 mg/g for Cr (VI) (Zhao et al., 2005), soil (9.5 mg/g for phenol (Subramanyam and Das, 2009, Păcurariu et al., 2013)). and carbon nanotubes (12.5 mg/g for Cr (VI) (Huang et al., 2015)). Li et al. (2015) also reported adsorption capacities within our range for the removal of Cr (VI) using Zeolitic imidazolate framework-67 micro-crystals. They reported 5.9, 9.3 and 13.3 mg/g for initial solutions of 6, 10 and 15 mg/L respectively. The adsorption capacities from the present study were higher than 3 adsorbents reported by (Mekonnen et al., 2015), namely avocado kernel seeds (1.0 mg/g), Juniperus procera saw dust (1.3 mg/g) and papaya peels (0.8 mg/g).

3.5. Adsorption kinetics

The kinetic experimental data was fitted to the models represented in equations (7) to (10). The results are shown in Fig. 6. The parameters of pseudo first order, pseudo second order and the intra-particle diffusion model were obtained using linear plots and determining the slope and intercept whereas the parameters of Elovich's equation were obtained through the Solver function in excel 2013 by minimizing the error. The associated constants are shown in Table 2.

Both the pseudo first order and Elovich's equation did not adequately represent the experimental data. This is in agreement with the relatively low regression coefficient value, $R^2 < 0.99$ and the inconsistencies between the fitted q_e and experimental values. To determine the nature of diffusion, the intra-particle diffusion model was adopted for Cr (VI) and phenol respectively. Based on equation (10), a plot of $q_t vst^{0.5}$ is a straight line when the intra-particle diffusion is a rate-limiting step. In case the intra-particle diffusion is the sole rate-limiting step, the plot will pass through the origin. In this study however, this is not the case, suggesting that the kinetics could be dominated by film diffusion and intra-particle diffusion at the same time (Qiu et al., 2009, Gupta and Balomajumder, 2015). The pseudo second order model adequately depicts the kinetic behavior of the removal of these pollutants on EG. This implies that the removal process is predominately driven by chemisorption and also depends on the physiochemical interactions between the EG and respective pollutants (da Gama et al., 2018).

3.6. Thermodynamic modelling

An understanding of the thermodynamics of the system is necessary in order to deduce if a process is spontaneous, endothermic or not. To determine this, non-linear isotherms of adsorption at three predetermined temperatures were conducted. Using the best fitting model, an equilibrium constant was obtained for the respective temperatures. The corresponding thermodynamic parameters of adsorption were obtained using the Van't Hoff's equation (12) which measures the changes in equilibrium constants with variations of the temperature. A graph of $\ln Ke$ vs 1/T was constructed to determine the values of the standard enthalpy change (ΔH^o) and standard entropy change (ΔS^o) from the slope and intercept of the linear

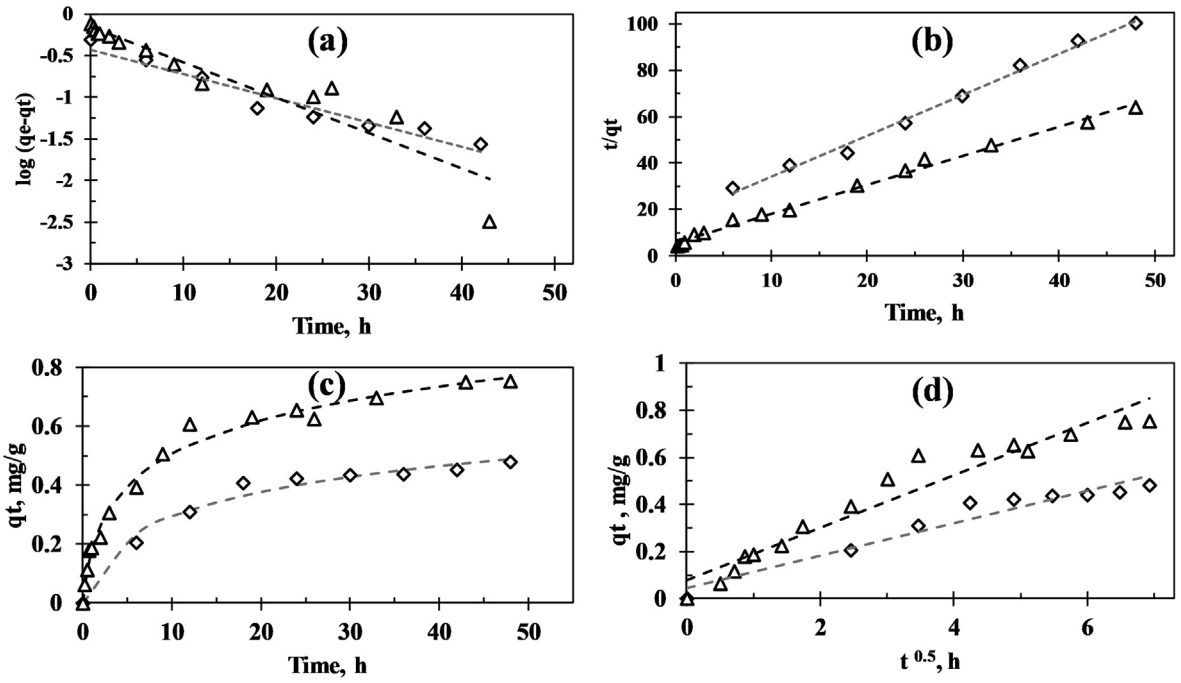

Fig. 6 Kinetic data fits using (a) pseudo first order (b) pseudo second order (c) Elovich's equation (d) Intra-particle diffusion model. The triangles (Δ) represents raw data for Cr (VI) and the diamond (◇) represents the raw data for phenol. The dashed lines represent the model fits for the respective models.

Table 2 Parameters derived from the various kinetics models.

	Pseudo first order			Pseudo second order			Elovich's equation			Intra-particle diffusion		
	k_{p1}	q_e	R^2	k_{p2}	qe	R^2	*a*	α	R^2	k_{int}	I	R^2
Cr (VI)	0.098	0.689	0.894	0.289	0.798	0.993	0.318	5.879	0.989	0.111	0.079	0.938
Phenol	0.067	0.373	0.942	0.191	0.566	0.992	0.106	7.502	0.980	0.069	0.045	0.934

Table 3 Thermodynamic parameters for the adsorption of Cr (VI) and Phenol on EG.

Component	Temperature (K)	$\Delta G^o(\frac{kJ}{mol})$	$\Delta H^o(\frac{kJ}{mol})$	$\Delta S^o(\frac{kJ}{mol})$
Cr (VI)	323	−31.24	46.57	240.52
	343	−28.64		
	363	−29.10		
Phenol	323	−20.47	4.96	88.90
	343	–22.42		
	363	–23.82		

plot while the standard Gibb's free energy change (ΔG^o) was determined using equation (13) where

$$\ln K_e = \frac{-\Delta H^o}{RT} + \frac{-\Delta S^o}{R} \tag{12}$$

T is the absolute temperature (K), R is the universal gas constant (8.314 J/ K.mol) and K_e is the thermodynamic equilibrium constant.

$$\Delta G^o = -\mathrm{RT} \ln Ke \tag{13}$$

The equilibrium constant obtained in the respective isotherms was expressed in the units (L/mg) and was converted to a dimensionless constant (K_e) using the method detailed by (Lima et al., 2019).

The thermodynamic study of both phenol and Cr (VI) adsorption resulted in positive values ofΔH^o indicating an endothermic adsorption process (Table 3). The negative values ofΔG^o at all temperatures for both pollutants indicated a spontaneous and a feasible process. High positive values ofΔS^o particularly for Cr (VI) were obtained, this reflects a high affinity

of EG towards the respective pollutants. The positive ΔS^o values also indicate increased randomness in the solid–liquid interface and increased degree of freedom of the sorbate and a favorable adsorption process (Ghosal and Gupta, 2017).

4. Conclusion

Exfoliated graphite efficiently removed phenol and Cr (VI) from an aqueous system. Equilibrium was attained within 48 h and approximately 90% of Cr (VI) was removed while 60% of the phenol was adsorbed in the same duration. The maximum amount of Cr (VI) was removed in the acidic region conditions whereas the maximum amount of phenol was removed in the basic region. The removal mechanism of Cr (VI) was accurately predicted by the non-linear Langmuir equation while the non-linear Redlich-Peterson equation accurately predicted the phenol removal. The pseudo-second order rate equation adequately represented the raw data for phenol and Cr (VI) with regression coefficients higher than 0.99. The thermodynamic parameters and the standard Gibbs free energy were calculated for phenol and Cr (VI). The standard Gibbs free energy values confirmed how feasible and spontaneous the adsorption process, while the change in enthalpy and change in entropy showed an endothermic process with some randomness.

Declaration of Competing Interest

The authors declare that they have no known competing financial interests or personal relationships that could have appeared to influence the work reported in this paper.

Acknowledgement

This work is based on the research supported in part by the National Research Foundation of South Africa (Grant Numbers: 117905).

References

Akram, M., Bhatti, H.N., Iqbal, M., Noreen, S., Sadaf, S., 2017. Biocomposite efficiency for Cr (VI) adsorption: Kinetic, equilibrium and thermodynamics studies. J. Environ. Chem. Eng 5, 400–411. https://doi.org/10.1016/j.jece.2016.12.002.

Aksu, Z., Akpinar, D., 2000. Simultaneous adsorption of phenol and chromium (VI) from binary mixtures onto powdered activated carbon. J. Environ. Sci. & Health A. 35, 379–405. https://doi.org/10.1080/10934520009376977.

Belhchemi, M., Addoun, F., 2011. Comparative adsorption isotherms and modeling of methylene blue onto activated carbons. Appl. Water Sci. 1, 111–117. https://doi.org/10.1007/s13201-011-0014-1.

Carvallho, M.N., Da Silva, K.S., Sales, D.C., Freire, E.M., Sobrinho, M.A., Ghislandi, M.G., 2016. Dye removal from textile industrial effluents by adsorption on exfoliated graphite nanoplatelets: kinetic and equilibrium studies. Water Sci. and Technol. 73, 2189–2198. https://doi.org/10.2166/wst.2016.073.

Chung, D.D.L., 2015. A review of exfoliated graphite. J. Mater. Sci. 51, 554–568. https://doi.org/10.1007/s10853-015-9284-6.

Da Gama, B.M.V., Do Nascimento, G.E., Sales, D.C.S., Rodriguez-Diaz, J. M., Barbosa, Menezes, C.M.B., Duarte, M.M.M.B. 2018. Mono and binary component adsorption of phenol and cadmium using adsorbent derived from peanut shells. J. Clean. Prod. 201, 219-228. DOI: 10.1016/j.jclepro.2018.07.291

Dehghani, M.H., Sanaei, D., Ali, I., Bhatnagar, A., 2016. Removal of chromium (VI) from aqueous solution using treated waste newspaper as a low-cost adsorbent: kinetic modeling and isotherm studies. J. Mol. Liq. 215, 671–679. https://doi.org/10.1016/j.molliq.2015.12.057.

Desta, M.B., 2013. Batch sorption experiments: Langmuir and Freundlich isotherm studies for the adsorption of textile metal ions onto teff straw (Eragrostis tef) agricultural waste. J. Thermodyn. 2013. https://doi.org/10.1155/2013/375830.

Diao, Z.H., Xu, X.R., Jiang, D., Kong, L.J., Sun, Y.X., Hu, Y.X., Hao, Q.W., Chen, H., 2016. Bentonite-supported nanoscale zero-valent iron/persulfate system for the simultaneous removal of Cr (VI) and phenol from aqueous solutions. Chem. Eng. J. 302, 213–222. https://doi.org/10.1016/j.cej.2016.05.062.

Ferrero, F., Tonetti, C., Periolatto, M., 2014. Adsorption of chromate and cupric ions onto chitosan-coated cotton gauze. Carbohydr. Polym. 110, 367–373. https://doi.org/10.1016/j.carbpol.2014.04.016Focke, W.W., Badenhorst, H., Mhike, W., Kruger, H.J., Lombaard, D. 2014. Characterization of commercial expandable graphite fire retardants. Thermochim. Acta, 584, 8-16. DOI: 10.1016/j.tca.2014.03.021.

Focke W, W, Badenhorst, H, Mhike, W, Kruger J, H, 2014. Characterization of commercial expandable graphite fire retardants. Thermochim. Acta 584, 8–16. https://doi.org/10.1016/j.tca.2014.03.021.

Foo, K.Y., Hameed, B.H., 2010. Insights into the modeling of adsorption isotherm systems. Chem. Eng. J. 156, 2–10. https://doi.org/10.1016/j.cej.2009.09.013.

Garg, U.K., Kaur, M., Garg, V., Sud, D., 2007. Removal of hexavalent chromium from aqueous solution by agricultural waste biomass. J. Hazard. Mater. 140, 60–68. https://doi.org/10.1016/j.jhazmat.2006.06.056.

Ge, M., Wang, X., Du, M., Liang, G., Hu, G., SM, J.A. 2019. Adsorption analyses of phenol from aqueous solutions using magadiite modified with organo-functional groups: Kinetic and equilibrium studies. Materials, 12, 96. doi: 10.3390/ma12010096

Ghosal, P.S., Gupta, A.K., 2017. Determination of thermodynamic parameters from Langmuir isotherm constant-revisited. J. Mol. Liq. 225, 137–146. https://doi.org/10.1016/j.molliq.2016.11.058.

Gimbert, F., Morin-Crini, N., Renault, F., Badot, P.M., Crini, G., 2008. Adsorption isotherm models for dye removal by cationized starch-based material in a single component system: error analysis. J. Hazard. Mater. 157, 34–46. https://doi.org/10.1016/j.jhazmat.2007.12.072.

Gladysz-Plaska, A., Majdan, M., Pikus, S., Sternik, D., 2012. Simultaneous adsorption of chromium (VI) and phenol on natural red clay modified by HDTMA. Chem. Eng. J. 179, 140–150. https://doi.org/10.1016/j.cej.2011.10.071.

Gupta, A., Balomajumder, C., 2015. Simultaneous adsorption of Cr (VI) and phenol onto tea waste biomass from binary mixture: multicomponent adsorption, thermodynamic and kinetic study. J. Environ. Chem. Eng. 3, 785–796. https://doi.org/10.1016/j.jece.2015.03.003.

Huang, J., Wang, X., Jin, Q., Liu, Y., Wang, Y., 2007. Removal of phenol from aqueous solution by adsorption onto OTMAC-modified attapulgite. J. Environ. Manage. 84, 229–236. https://doi.org/10.1016/j.jenvman.2006.05.007.

Huang, Y., Ma, X., Liang, G., Yan, H., 2008a. Adsorption of phenol with modified rectorite from aqueous solution. Chem. Eng. J. 141, 1–8. https://doi.org/10.1016/j.cej.2007.10.009.

Huang, Y., Ma, X., Liang, G., Yan, Y., Wang, S., 2008b. Adsorption behavior of Cr (VI) on organic-modified rectorite. Chem. Eng. J. 138, 187–193. https://doi.org/10.1016/j.cej.2007.06.017.

Huang, Z.N., Wang, X.L., Yang, D.S., 2015. Adsorption of Cr (VI) in wastewater using magnetic multi-wall carbon nanotubes. Water Sci. Eng. 8, 226–232. https://doi.org/10.1016/j.wse.2015.01.009.

Ji, L., Chen, W., Duan, L., Zhu, D., 2009. Mechanisms for strong adsorption of tetracycline to carbon nanotubes: a comparative

study using activated carbon and graphite as adsorbents. Environ. Sci. Technol. 43, 2322–2327. https://doi.org/10.1021/es803268b.

Kumar, K.V., Porkodi, K., Rocha, F., 2008. Isotherms and thermodynamics by linear and non-linear regression analysis for the sorption of methylene blue onto activated carbon: comparison of various error functions. J. Hazard. Mater. 151, 794–804. https://doi.org/10.1016/j.jhazmat.2007.06.056.

Kundu, S., Gupta, A., 2006. Arsenic adsorption onto iron oxide-coated cement (IOCC): regression analysis of equilibrium data with several isotherm models and their optimization. Chem. Eng. J. 122, 93–106. https://doi.org/10.1016/j.cej.2006.06.002.

Li, X., Ai, L., Jiang, J., 2016. Nanoscale zerovalent iron decorated on graphene nanosheets for Cr (VI) removal from aqueous solution: surface corrosion retard induced the enhanced performance. Chem. Eng. J. 288, 789–797. https://doi.org/10.1016/j.cej.2015.12.022.

Li, Y., Du, Q., Liu, T., Sun, J., Jiao, Y., Xia, Y., Xia, L., Wang, Z., Zhang, W., Wang, K., 2012. Equilibrium, kinetic and thermodynamic studies on the adsorption of phenol onto graphene. Mater. Res. Bull. 47, 1898–1904. https://doi.org/10.1016/j.materresbull.2012.04.021.

Li, X., Gao, X., Ai, L., Jiang, J., 2015. Mechanistic insight into the interaction and adsorption of Cr (VI) with zeolitic imidazolate framework-67 microcrystals from aqueous solution. Chem. Eng. J. 274238–246. https://doi.org/10.1016/j.cej.2015.03.127.

Liang, H., Song, B., Peng, P., Jiao, G., Yan, X., She, D., 2019. Preparation of three-dimensional honeycomb carbon materials and their adsorption of Cr (VI). Chem. Eng. J. 3679–16. https://doi.org/10.1016/j.cej.2019.02.121.

Lima, E.C., Hosseini-Bandegharaei, A., Moreno-Pirajan, J.C., Anastopoulos, I., 2019. A critical review of the estimation of the thermodynamic parameters on adsorption equilibria. Wrong use of equilibrium constant in the Van't Hoof equation for calculation of thermodynamic parameters of adsorption. J. Mol. Liq. 273, 425–434. https://doi.org/10.1016/j.molliq.2018.10.048.

Lütke, S.F., Igansi, A.V., Pegoraro, L., Dotto, G.L., Pinto, L.A., Cadaval Jr, T.R., 2019. Preparation of activated carbon from black wattle bark waste and its application for phenol adsorption. J. Environ. Chem. Eng. 7,. https://doi.org/10.1016/j.jece.2019.103396 103396.

Makrigianni, V., Giannakas, A., Deligiannakis, Y., Konstantinou, I., 2015. Adsorption of phenol and methylene blue from aqueous solutions by pyrolytic tire char: equilibrium and kinetic studies. J. Environ. Chem. Eng. 3, 574–582. https://doi.org/10.1016/j.jece.2015.01.006.

Mekonnen, E., Yitbarek, M., Soreta, T.R., 2015. Kinetic and thermodynamic studies of the adsorption of Cr (VI) onto some selected local adsorbents. S. Afr. J. Chem. 6845–52. https://doi.org/10.17159/0379-4350/2015/v68a7.

Meniai, A., 2012. The use of sawdust as by product adsorbent of organic pollutant from wastewater: adsorption of phenol. Energy Procedia 18905–914. https://doi.org/10.1016/j.egypro.2012.05.105.

Nagy, B., Manzatu, C., Maicaneanu, A., Indolean, C., Barbu-Tudoran, L., Majdik, C., 2017. Linear and nonlinear regression analysis for heavy metals removal using Agaricus bisporus macrofungus. Arab. J. Chem. 10, S3569–S3579. https://doi.org/10.1016/j.arabjc.2014.03.004.

Naidoo, S., Olaniran, A.O., 2013. Treated wastewater effluent as a source of microbial pollution of surface water resources. *Int.l.* J. Environ. Res. Public Health 11, 249–270. https://doi.org/10.3390/ijerph110100249.

Noel, M, Santhanam, R, 1998. Electrochemistry of graphite intercalation compounds. Journal of Power Sources 72, 53–65. https://doi.org/10.1016/S0378-7753(97)02675-X.

Păcurariu, C., Mihoc, G., Popa, A., Muntean, S.G., Ianoş, R., 2013. Adsorption of phenol and p-chlorophenol from aqueous solutions on poly (styrene-co-divinylbenzene) functionalized materials. Chem. Eng. J. 222218–227. https://doi.org/10.1016/j.cej.2013.02.060.

Qiu, H., Lv, L., Pan, B.C., Zhang, Q.J., Zhang, W.M., Zhang, Q.X., 2009. Critical review in adsorption kinetic models. J. Zhejiang Uni. Sci. A 10, 716–724. https://doi.org/10.1631/jzus.A0820524.

Rai, M., Shahi, G., Meena, V., Meena, R., Chakraborty, S., Singh, R., Rai, B. 2016. Removal of hexavalent chromium Cr (VI) using activated carbon prepared from mango kernel activated with H3PO4. Resource-Efficient Technologies, 2S63-S70. DOI: 10.1016/j.reffit.2016.11.011

Rakhunde, R., Deshpande, L., Juneja, H., 2012. Chemical speciation of chromium in water: a review. Crit. Rev. Environ. Sci. Technol. 42, 776–810. https://doi.org/10.1080/10643389.2010.534029.

Ravulapalli, S., Kunta, R., 2018. Enhanced removal of chromium (VI) from wastewater using active carbon derived from Lantana camara plant as adsorbent. Water Sci. Technol. 78, 1377–1389. https://doi.org/10.2166/wst.2018.413.

Samani, R.M., Ebrahimbabaie, P., Molamahmood, H.V., 2016. Hexavalent chromium removal by using synthesis of polyaniline and polyvinyl alcohol. Water Sci. Technol. 74, 2305–2313. https://doi.org/10.2166/wst.2016.412.

Senturk, H.B., Ozdes, D., Gundogdu, A., Duran, C., Soylak, M., 2009. Removal of phenol from aqueous solutions by adsorption onto organomodified Tirebolu bentonite: Equilibrium, kinetic and thermodynamic study. J. Hazard. Mater. 172, 353–362. https://doi.org/10.1016/j.jhazmat.2009.07.019.

Shahbeig, H., Bagheri, N., Ghorbanian, S.A., Hallajisani, A., Poorkarimi, S., 2013. A new adsorption isotherm model of aqueous solutions on granular activated carbon. World J. Model. Simul. 9, 243–254.

Singh, N., Kumari, A., Balomajumder, C., 2018. Modeling studies on mono and binary component biosorption of phenol and cyanide from aqueous solution onto activated carbon derived from saw dust. Saudi J. Biol. Sci. 25, 1454–1467. https://doi.org/10.1016/j.sjbs.2016.01.007.

Subramanyam, B., Das, A., 2009. Study of the adsorption of phenol by two soils based on kinetic and isotherm modeling analyses. Desalination 249, 914–921. https://doi.org/10.1016/j.desal.2009.05.020.

Szabó, M., Kalmár, J., Ditrói, T., Bellér, G., Lente, G., Simic, N., Fábián, I., 2018. Equilibria and kinetics of chromium (VI) speciation in aqueous solution–a comprehensive study from pH 2 to 11. Inorganica Chim. Acta. 472295–301. https://doi.org/10.1016/j.ica.2017.05.038.

Tang, H., Zhao, Y., Shan, S., Yang, X., Liu, D., Cui, F., Xing, B., 2018. Theoretical insight into the adsorption of aromatic compounds on graphene oxide. Environ. Sci. Nano. 5, 2357–2367. https://doi.org/10.1039/C8EN00384J.

Tichapondwa, S., Van Biljon, J., 2019. Adsorption of Cr (VI) Pollutants in Water Using Natural and Modified Attapulgite Clay. Chem. Eng. Trans. 74, 355–360. https://doi.org/10.3303/CET1974060.

Tichapondwa, S.M., Tshemese, S., Mhike, W., 2018. Adsorption of phenol and chromium (VI) pollutants in wastewater using exfoliated graphite. Chem. Eng. Trans. 70, 847–852. https://doi.org/10.3303/CET1870142.

Tshemese, S.J., Mlaba, T.T., Tichapondwa, S.M., Mhike, W., 2020. Removal of chromium (VI) from aqueous solution using exfoliated graphite/polyaniline composite. Chem. Eng. Trans. 81, 565–570. https://doi.org/10.3303/CET2081095.

Tshuto, T., Kitoto, E., Ranamane, L., Chirwa, E.M., 2017. Simultaneous Degradation of Phenol and Reduction of Chromium (VI) Using UV/TiO_2 Photocatalysis. Chem. Eng. Trans. 57, 895–900. https://doi.org/10.3303/CET1757150.

Van Pham, T., Van Tran, T., Nguyen, T.D., Tham, N.T.H., Quang, P. T.T., Uyen, D.T.T., Le, N.T.H., Vo, D.V.N., Thanh, N.T., Bach, L.G., 2019. Adsorption behavior of Congo red dye from aqueous solutions onto exfoliated graphite as an adsorbent: Kinetic and isotherm studies. Mater. Today 18, 4449–4457. https://doi.org/10.1016/j.matpr.2019.07.414.

Van Pham, T., Van Tran, T., Nguyen, T.D., Tham, N.T.H., Quang, P. T.T., Uyen, D.T.T., Le, N.T.H., Vo, D.V.N., Thanh, N.T., Bach, L.G., 2020. Development of Response Surface Methodology for Optimization of Congo Red Adsorption Utilizing Exfoliated Graphite As An Efficient Adsorbent. Mater. Today 22, 2341–2350. https://doi.org/10.1016/j.matpr.2020.03.356.

Wang, X., Huang, S., Zhu, L., Tian, X., Li, S., Tang, H., 2014. Correlation between the adsorption ability and reduction degree of graphene oxide and tuning of adsorption of phenolic compounds. Carbon 69101–112. https://doi.org/10.1016/j.carbon.2013.11.070.

Won, Y.-J., Lee, J., Choi, D.-C., Chae, H.R., Kim, I., Lee, C.-H., Kim, I.-C., 2012. "Preparation and application of patterned membranes for wastewater treatment" *Environ*. Sci. Technol. 46, 11021–11027. https://doi.org/10.1021/es3020309.

Wong, Y., Szeto, Y., Cheung, W., Mckay, G., 2004. Adsorption of acid dyes on chitosan—equilibrium isotherm analyses. Process Biochem. 39, 695–704. https://doi.org/10.1016/S0032-9592(03)00152-3.

Yu, S., Wang, X., Yao, W., Wang, J., Ji, Y., Ai, Y., Alsaedi, A., Hayat, T., Wang, X., 2017. Macroscopic, spectroscopic, and theoretical investigation for the interaction of phenol and naphthol on reduced graphene oxide. Environ. Sci. Technol. 51, 3278–3286. https://doi.org/10.1021/acs.est.6b06259.

Yu, W., Zhang, L., Wang, H., Chai, L., 2013. Adsorption of Cr (VI) using synthetic poly (m-phenylenediamine). J. Hazard. Mater. 260789–795. https://doi.org/10.1016/j.jhazmat.2013.06.045.

Zhao, N., Wei, N., Li, J., Qiao, Z., Cui, J., He, F., 2005. Surface properties of chemically modified activated carbons for adsorption rate of Cr (VI). Chem. Eng. J. 115, 133–138. https://doi.org/10.1016/j.cej.2005.09.017.